



NECESSITY AND TECHNIQUES OF MITIGATION OF URBAN HEAT ISLAND (UHI) INTENSITY OF KANPUR METROPOLIS IN THE GANGA-YAMUNA DOAB REGION OF INDIA

¹Himanshu Gandhi, ²G.L. Srivastava ³Vikram Gauarv Singh, ⁴Shiv Bahadur Singh, ⁵Vinay Kumar

¹Research Scholar, ²Professor, ³Coordinator, ⁴Research Scholar, ⁵Research Scholar

¹Department of Geography, ²Department of Geography, ³Source Sustainability at State Water and Sanitation Mission UP, ⁴Department of Geography, ⁵Department of Geography

¹DAV Degree College, Kanpur, India, ²DAV Degree College, Kanpur, India, ³Aga Khan Foundation, Lucknow, India, ⁴VSSD College, Kanpur, India, ⁵DAV Degree College, Kanpur, India

Abstract: Urban environment alters biophysical mechanisms causes a change in surface to atmosphere temperature and forms storage heat flux (ΔQ_s) and releases as sensible heat flux which in turn forms Urban Heat Island (UHI) Intensity. So, the impact of UHI Intensity on human health and ecological evolution should be studied in a developing nation like India having a large young population and a diverse range of species. With this in mind, it is also necessary to examine the UHI Intensity mitigation processes. The current study examined the impact of UHI Intensity on human health and ecological evolution in Kanpur Metropolis, which is located on the banks of the Ganga but now/will, occupies/occupy the area of Kanpur Nagar District with the Yamuna River serving as the region's southern boundary due to urban sprawl. Urban Heat Island (UHI) Intensity Discomfort Index (DI) and Urban Thermal Field Variation Index (UTFVI) has been carried out for this region with projection WGS_1984_UTM_Zone_44N using Landsat 5, 7 & 8 data for the years 1991, 2001, 2011 & 2021 respectively. The best fit curve with a logarithmic trendline shows a positive correlation between UHI intensity and DI and UTFVI, which has been evaluated. The significant level (p) for DI and UTFVI was also evaluated, and the p value of $<.005$ was found to be satisfactory. This indicates that the severity of UHI intensity has a significant impact on human discomfort and ecological evolution. The study also offers insightful information about the policy-making processes involved in urban planning, such as how to create green and blue spaces and other human made infrastructures during urban spatial planning for UHI intensity mitigation.

Key words: Ecological evolution, Discomfort, Green space, Blue space

Introduction:

More than half of the earth's human population, i.e., 55%, already lives in urban areas, and this number is expected to increase up to 68% by 2050 (UN, 2019). (Mirzaei, 2015; Morris et al., 2015) showed that the rapid growth and wide-ranging impact of urban areas give rise to numerous urban issues, many of which UHI is biggest one and has its own concern. In fact, UHI is a phenomenon closely related with the development of cities and urban expansions (Yeeyong Lee et al., 2014). Measurement of Surface UHI intensity which is based on several empirical studies (Johnson 1985; Hogan and Ferrick 1998; Klysik, Fortuniak and Steinecke 1999; Morris et al. and Unger et al., 2001; Zhao et al., 2014), which is based on the measurement of land-surface temperatures (LST) that directly affect air temperature in the canopy layer by energy exchange changes in urban environments. According to Hart and Sailor (2009) and Holmer, Kjellstrom and Lemke (2009), this type of urban background climate and its heat formation have an impact on human health (Nidhi Singh et al., 2020) as well as outdoor working conditions and productivity. People experience discomfort (Toy, Yilmaz, and Yilmaz, 2007), which can be measured by the Discomfort Index (DI) (José Antonio Sobrino and Itziar Irakulis, 2020). (Ihara, Kusaka, Hara, Matsuhashi, & Yoshida, 2011) found that thermal comfort at night is essential for restful sleep while the Urban Thermal Field Variance Index (UTFVI) phenomenon can be used to quantitatively and qualitatively description of the SUHI intensity effect's vulnerability (Tomlinson et al. 2011; Kafy et al. 2021; Md. Nazmul Huda Naim et al., 2021). As the Surface Urban Heat Island (SUHI) effect affects in the form of decreased comfort and an increase in mortality rate (Sejati et al., 2019), as well as having an impact on ecological evolution (Liu, L., Zhang Y., 2011; Renard Florent et al., 2019) as it effects animals, vegetation and other living and non-living things. In now-a-days, the Urban Thermal Field Variance Index (UTFVI) becomes a widely used index to more precisely describe the SUHI effect.

In order to study thermal anomalies like UHI in urban areas, researchers from all over the world are currently using satellite thermal imageries, particularly high resolution imagery. This type of imagery has the advantage of offering a repeatable dense grid of temperature data over an entire city.

According to a recent UN report (2019), China and India will account for more than one third of the rise in the world's urban population between 2014 and 2050. India has also experienced rapid urbanization recently. The main characteristics of Indian urbanization are unpredictable and uncontrolled urban growth with increases in impervious area and haphazard development. The area under artificial surfaces (e.g., urban and associated areas) has increased significantly in India between 1992 and 2020. Due to its abundant agricultural and hydrological resources, the Gangetic plains (GP) in India have seen more urbanization recently than other parts of the nation, and as a result, this region has been experiencing heat island intensity for a long time (Tirthankar Chakraborty et al., 2016; Meenu Rani et al., 2018).

The study is based on the use of Earth Observation (EO) datasets and a quantitative geospatial technology (GT) approach to identify UHI Intensity and its impact on ecological evolution and human health. This study also offers helpful advice on how to plan urban green space (Yiding et al., 2006) and blue space (Coutts et al., 2012) for urban development planning strategies and for reducing the effects of UHI in cities of developing nations like India.

Study Area:

In "Survey of India's" Toposheet Nos. 54N and 63B, the study area Kanpur Nagar District (Fig. 1) is situated over north-central India in the middle of the state of Uttar Pradesh between latitudes 25°55'N to 27°N and longitude 79°30'E to 80°35'E. With the Ganga River to the north-east and the Yamuna River to the south-west, it is the 11th most populous urban area in India. It is one of the Indian cities with a population of more than 4.5 million and serious socioeconomic and environmental problems.

The districts of Kanuuaj and Hardoi, Unnao in the east, Fatehpur and Hamirpur in the south, and Kanpur dehat in the west form its northern, eastern, southern, and western boundaries. It is separated from the districts of Kanpur dehat and Fatehpur in the west and south, respectively, by the Pandu River, and it is divided from district Unnao in the east by the holy Ganga River, which acts as a natural barrier. The Kanpur Nagar is part of the Smart City Project, Ministry of Housing and Urban Affairs, Government of India (GoI). The Kanpur Nagar district has a total area of 3180 sq. km, and the city's total area is 403 sq. km. It has a population of 4.58 million, with a density of 6850 people per km² (District Census Handbook, 2011) and have 6 statutory and 4 census towns. The study area is located on almost a flat plain with some minor undulations with the master slope from northwest to south-east, and the average elevation of land surface is 125 meters above mean sea level along with the rivers Ganga and Yamuna which forms the north-east and south-west boundaries of the study area, respectively, and develop the fertile agricultural hinter land of Ganga and Yamuna Doab. The district's sub-humid climate is marked by a hot summer and general dryness, with the exception of the south-west monsoon, and mean monthly maximum temperatures of 32.2°C and 19.5°C. The district receives an average annual rainfall of 821.9 mm. The main sedimentary components of the area are clay, silt, gravel, and sands of various grades, and the soil of the district displays a great variety in composition and appearance. The district also enjoys strong administration and has good range of all facilities for its people.

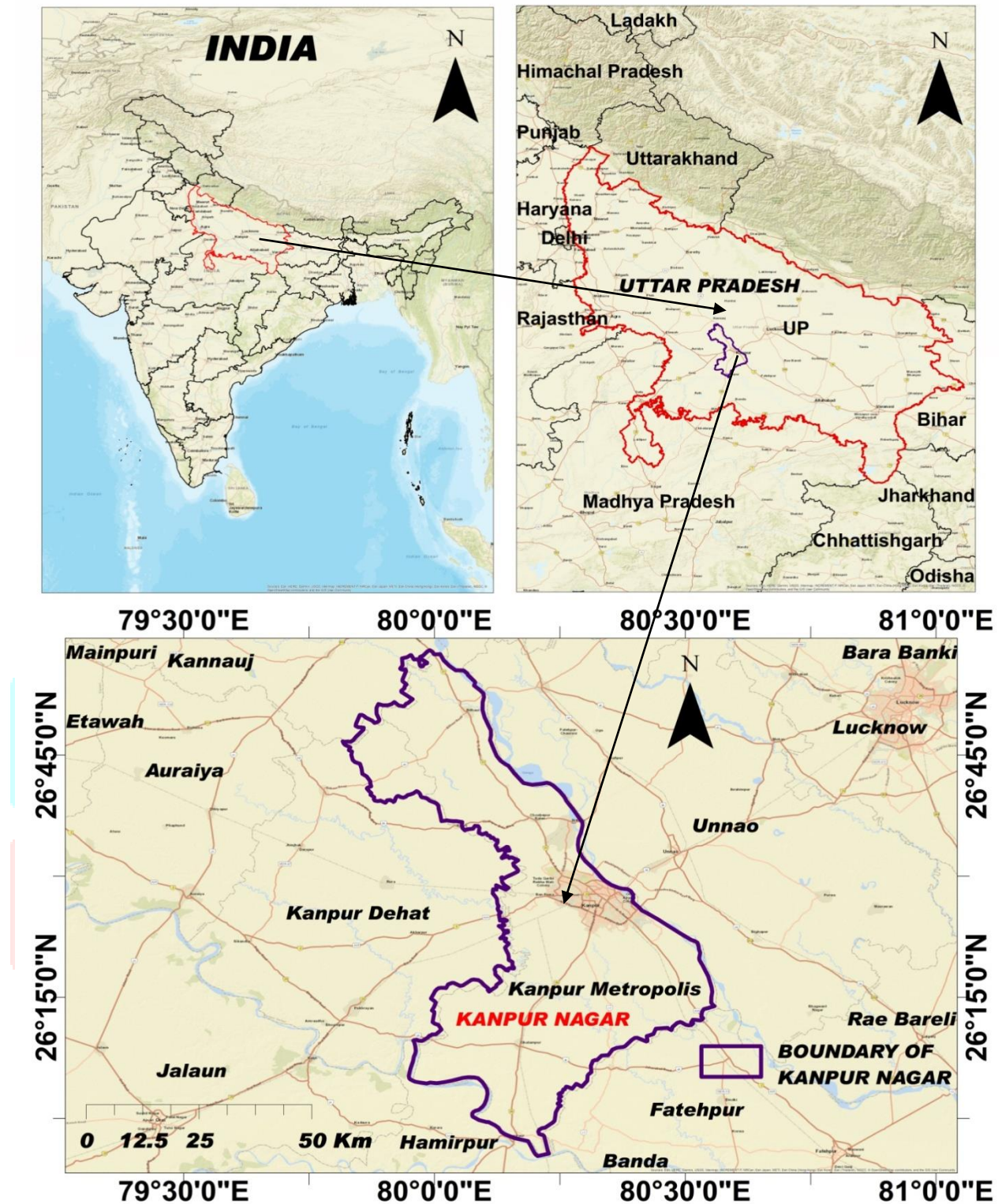


Figure 1

The district boundary of Kanpur Nagar and its surrounding areas are shown on the location map of the study area in Figure 1

Data:

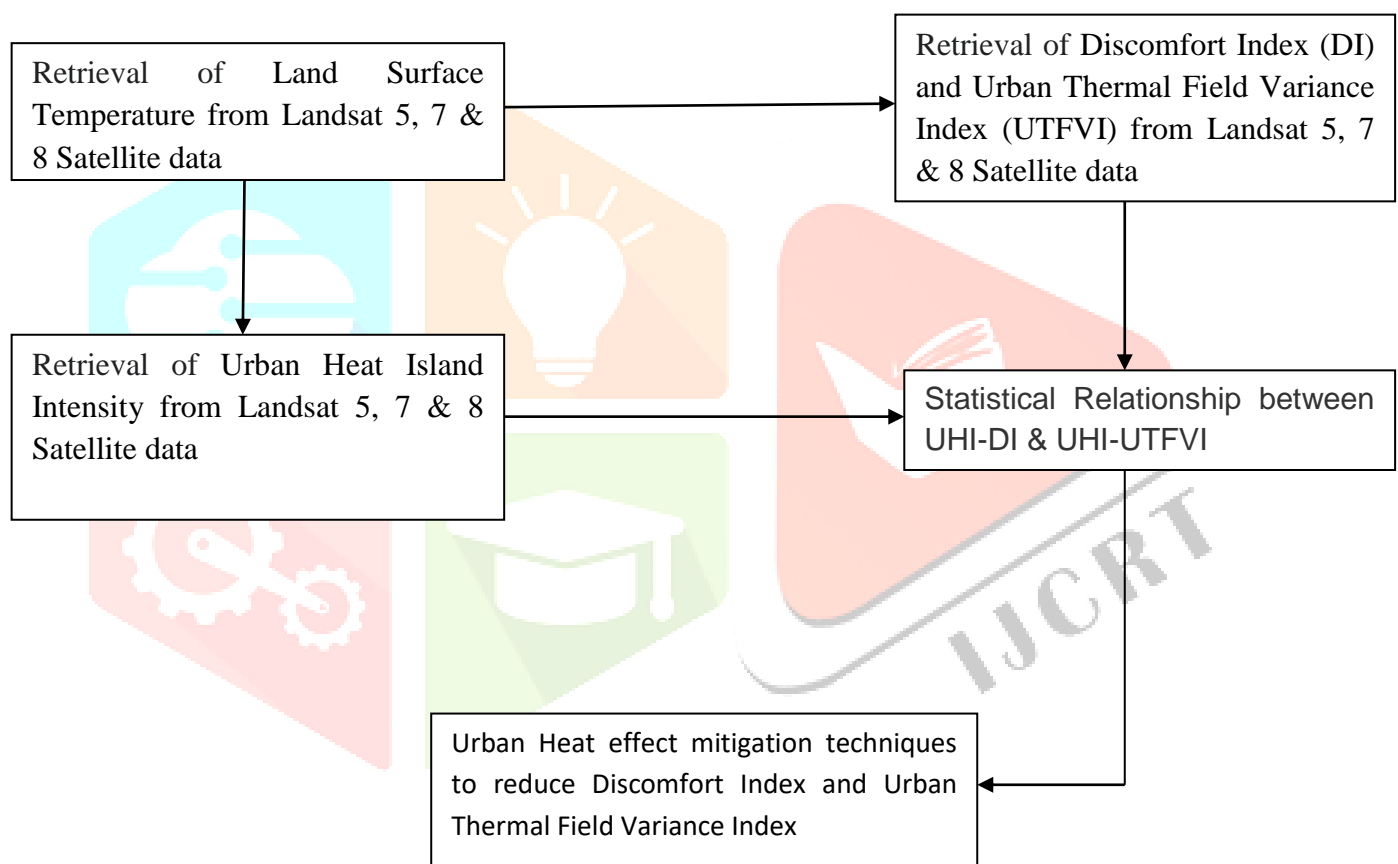
From the US Geological Survey's website, <https://earthexplorer.usgs.gov/>, path 144 and rows 041 and 042 of Landsat5, Landsat7, and Landsat8 data are downloaded. The data are then mosaiced, and ArcMap 10.8 software is used to extract data for the region.

Specifics of the used satellite images

Satellite	Sensor	Acquisition date	Path and row	Spatial resolution	Thermal resolution	Cloud Cover
Landsat 5	TM	16 March 1991	144/041 & 144/042	30 m	120(30)m	<10%
Landsat 7	ETM+	03 March 2001	144/041 & 144/042	30 m	60(30)m	<10%
Landsat 5	TM	07 March 2011	144/041 & 144/042	30 m	120(30)m	<10%
Landsat 8	OLI/TIRS	02 March 2021	144/041 & 144/042	30 m	100m	<10%

Methodology:

In this study, the UHI Intensity, Discomfort Index and Urban Thermal Field Variance Index were calculated from satellite images from the Landsat series, and the year-by-year values of each were compared to the DI and UTFVI. The methodology flow chart below provides a detailed explanation of the steps that were taken for the study.



2.3.1 Steps involved in Retrieval of Land Surface Temperature:

Step^{1st}: Convert the DN value to the at-sensor spectral radiance in the first step:

L is equal to $(L_{\max} - L_{\min}) \cdot Q_{\text{cal}} / (Q_{\text{calmax}} - Q_{\text{calmin}}) + L_{\min} + O_i$

Where,

L_{\max} is the maximum radiance in $\text{Wm}^{-2}\text{sr}^{-1}\mu\text{m}^{-1}$

L_{\min} is the minimum radiance in $\text{Wm}^{-2}\text{sr}^{-1}\mu\text{m}^{-1}$

Q_{cal} is the pixel's DN value

Q_{calmax} is the highest pixel DN value.

Q_{calmin} is the minimum DN value of pixels

O_i is correction value of the thermal band

Step 2nd: $T = K_2 / \ln(K_1 / L_\lambda + 1) - 273.15$

Where,

T is At - Kelvin (K) values of the satellite for the brightness temperature.

L is spectral radiation at the TOA (watts/(m²*ster*m)) at particular wavelength λ .

K_1 and K_2 are a constant for Band X, where X is the band number, and it stands for Band Specific Thermal Conversion from the Metadata.

Step 3rd: Calculation of Normalized Difference Vegetation Index (NDVI)

NDVI equals to $(NIR - RED) / (NIR + RED)$

Step 4th: Proportional vegetation (Pv) calculation:

P_V can be calculated as $((NDVI - NDVI_{min}) / (NDVI_{max} - NDVI_{min}))^2$

Step 5th: Emissivity calculation:

$\epsilon_\lambda = \epsilon_{v\lambda} P_V + \epsilon_{s\lambda} (1 - P_V)$

Where, P_V is the percentage of vegetation and ϵ_v and ϵ_s are the emissivities from the soil and vegetation respectively, at a given wavelength λ .

Step 6th: LST is equal to $BT / [1 + \lambda * (BT / \rho) * \ln(\epsilon)]$

Where, BT is brightness temperature, LST in degrees Celsius, ρ is (hc/σ) where σ being the Boltzmann constant (1.38×10^{-23} J/K), h being Plank's constant (6.626×10^{-34}), and c being the speed of light (3×10^8 m/s)

2.3.2 Discomfort Index Retrieval:

In 2020 Sobrino and Irakulis proposed that Discomfort Index can be used for the human restless conditions and it can be given as following empirical formula:

$$DI = LST - (0.55 - 0.0055 RH) (LST - 14.5)$$

Since relative humidity depends on land surface emissivity, it can also be described by water vapor content (WVC), where DI stands for discomfort index, LST for land surface temperature, and RH for relative humidity.

2.3.3 Urban Thermal Field Variance Index Retrieval:

Zhang et al., (2006) and K. Singh et al., (2017) state that it can be given as:

UTFVI is equal to $((T_s - T_{Mean}) / T_{Mean})$

Where, T_s stands for land surface temperature and T_{Mean} for the region's mean LST.

2.3.4 Urban Heat Island Intensity Retrieval:

$$UHI = (LST + \delta)/2$$

Where, δ is the land surface temperature's standard deviation.

2.3.5 Plotting of Graphs:

Microsoft Excel 2007 was used to plot a scattered graph with a logarithmic trendline using 168 randomly generated points from the region.

3. Result:

Section 3.1

The Discomfort index is retrieved for the following years: 1991, 2001, 2011, and 2021 and displayed as maps having projection WGS_1984_UTM_Zone_44N

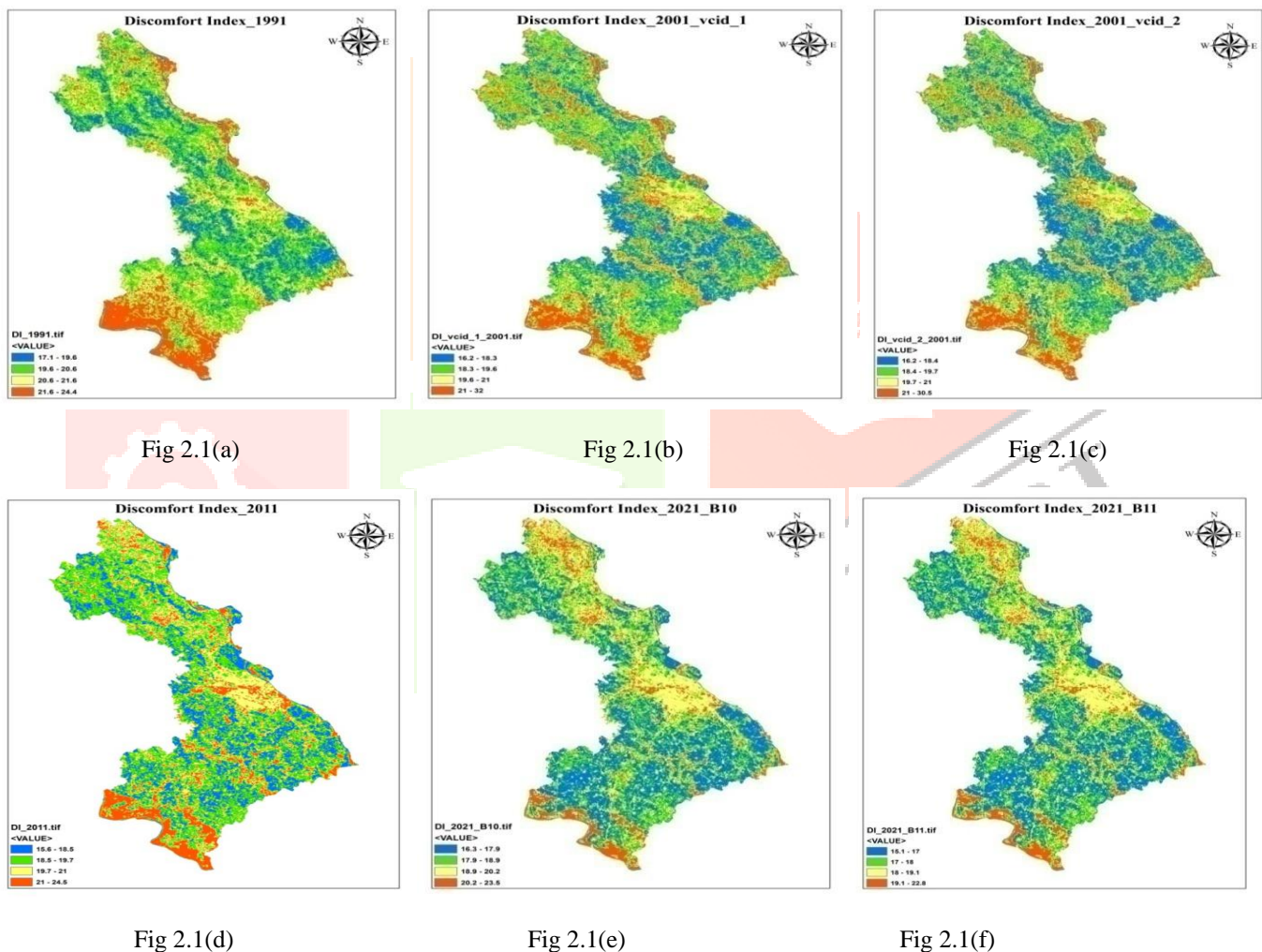


Figure 2.1(a) displays the Discomfort Index (DI) for 1991, Figure 2.1(b) and Figure 2.1(c) displays the DI for 2001 derived from vcid 1 and vcid 2, respectively, Figure 2.1(d) displays the DI for 2011, Figure 2.1(e) and Figure 2.1(f) displays the DI for 2021 derived from Band 10 and Band 11 respectively.

The study area region's UTFVI for 1991, 2001, 2011, and 2021 are retrieved, and they can be provided with projection WGS_1984_UTM_Zone_44N

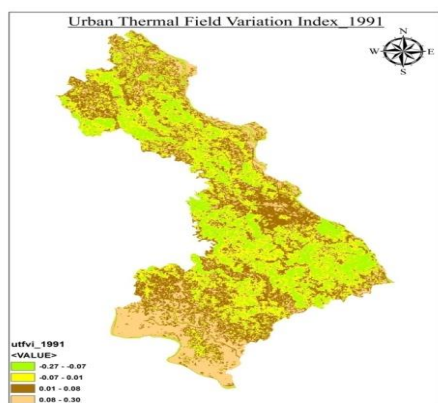


Fig 2.2(a)

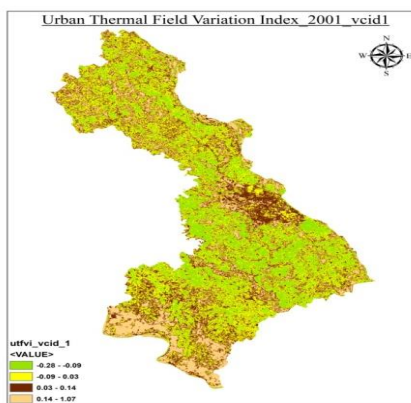


Fig 2.2(b)

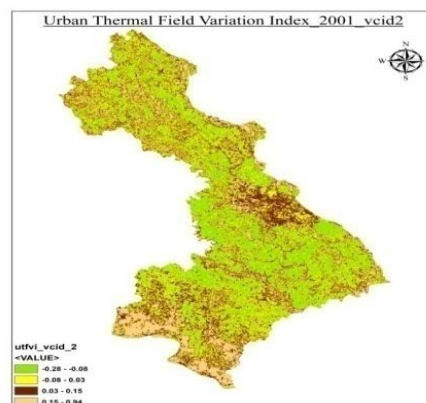


Fig 2.2(c)

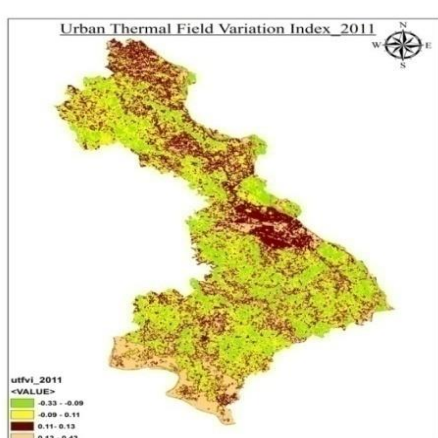


Fig 2.2(d)

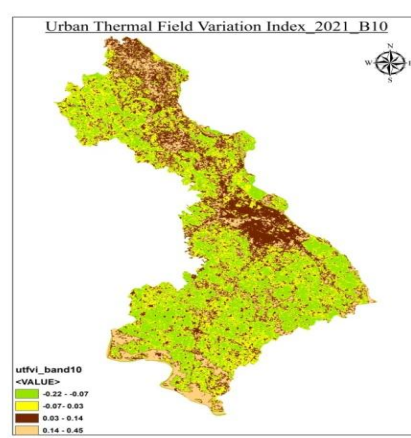


Fig 2.2(e)

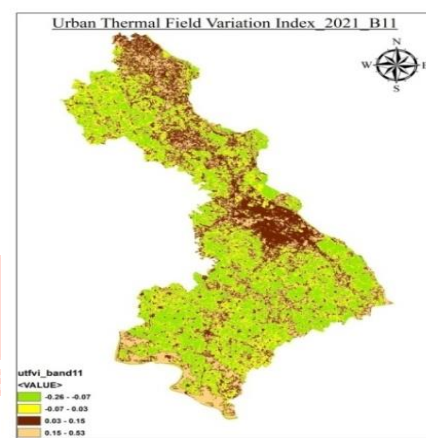


Fig 2.2(f)

Figure 2.2(a) displays the Urban Thermal Field Variance Index (UTFVI) for 1991, Figure 2.2(b) and Figure 2.2(c) displays the UTFVI for 2001 derived from vcid 1 and vcid 2 of thermal band respectively, Figure 2.2(d) displays the UTFVI for 2011, Figure 2.2(e) and Figure 2.2(f) displays the UTFVI for 2021 derived from Band 10 and Band 11 respectively.

Section 3.2

The study area region's UHI Intensity for 1991, 2001, 2011, and 2021 is retrieved, and it can be provided with projection WGS_1984_UTM_Zone_44N:

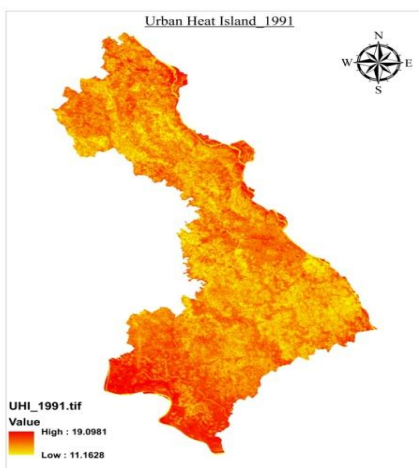


Figure 3.2(a)

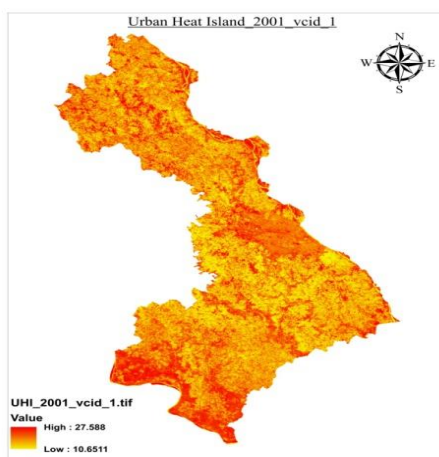


Figure 3.2(b)

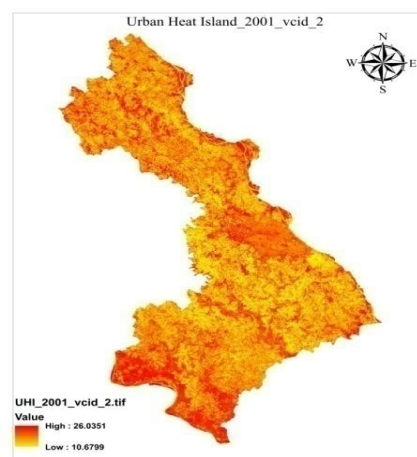


Figure 3.2(c)

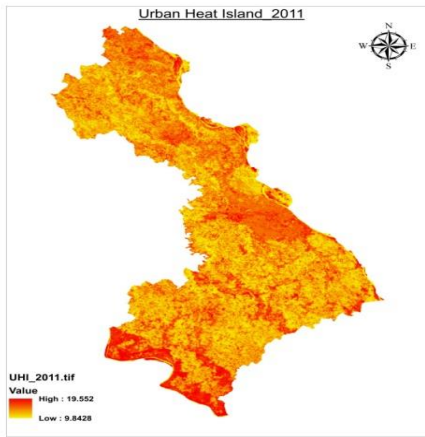


Figure 3.2(d)

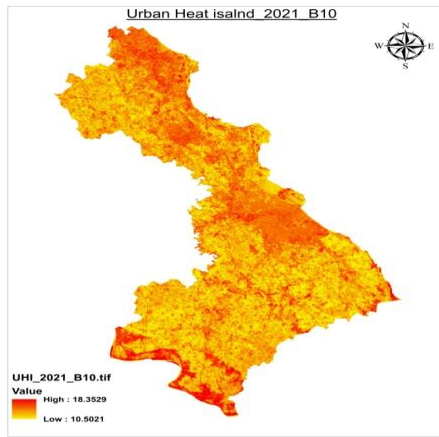


Figure 3.2(e)

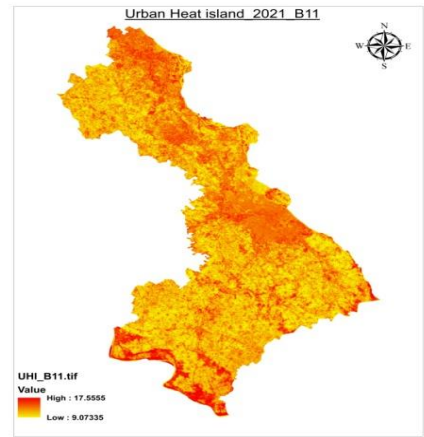
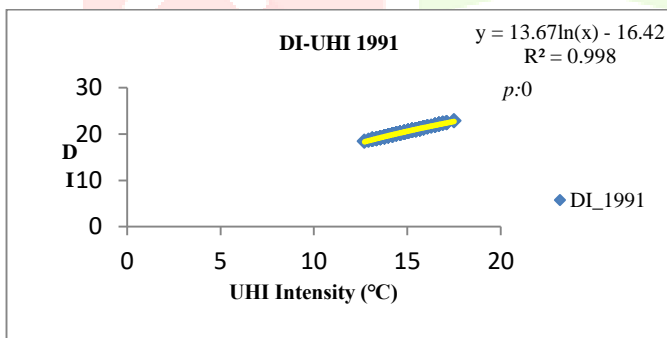


Figure 3.2(f)

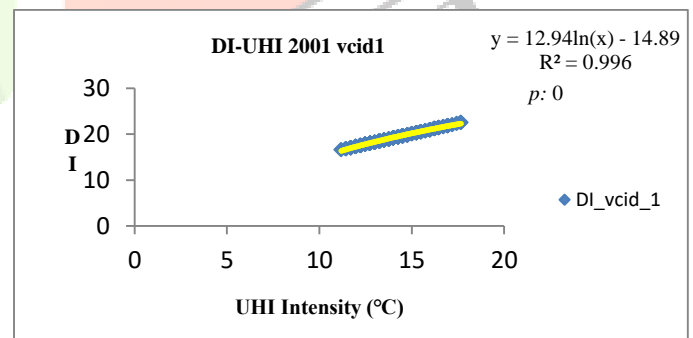
The Figure 3.2(a) shows the Urban Heat Island (UHI) Intensity for the 1991, Figure 3.2(b) and Figure 3.2(c) shows Urban Heat Island (UHI) Intensity for the 2001 derived from vcid 1 and vcid 2 of thermal band respectively, Figure 3.2(d) shows the Urban Heat Island (UHI) Intensity for 2011, Figure 3.2(e) and Figure 3.2(f) shows the Urban Heat Island (UHI) Intensity for 2021 derived from Band 10 and Band 11 respectively.

Section 3.3

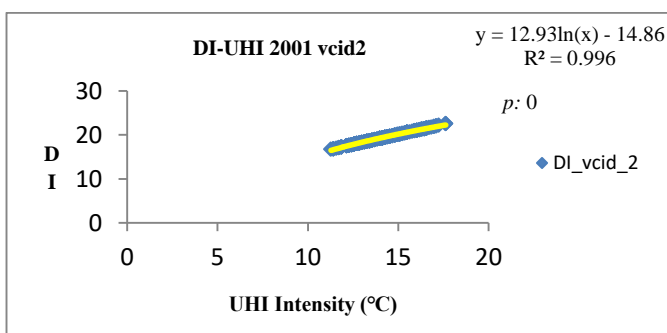
Because the value of the data in the area increases or decreases quickly, the Urban Heat Island (UHI) Intensity was compared with the Discomfort Index (DI) and Urban Thermal Field Variance Index (UTFVI) using 168 random points for the years 1991, 2001, 2011, and 2021. The results are plotted as the following graphs:



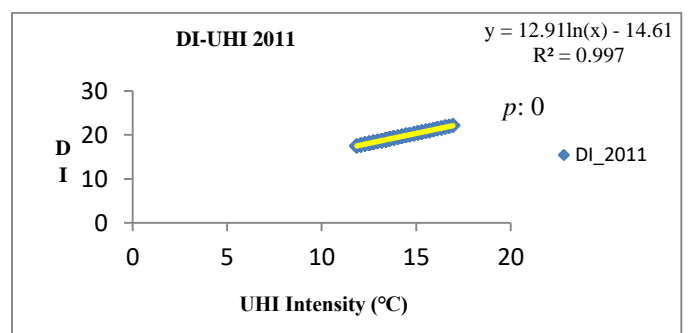
Graph 3.3.1(a)



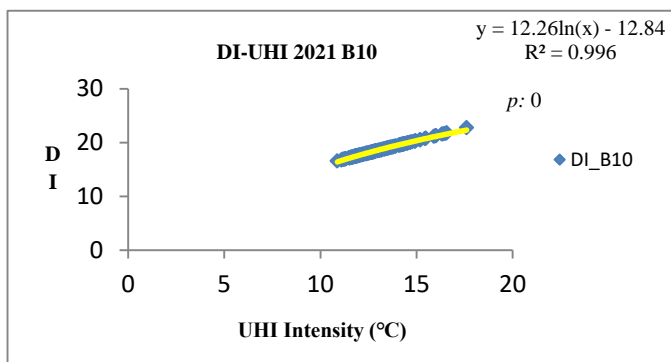
Graph 3.3.1(b)



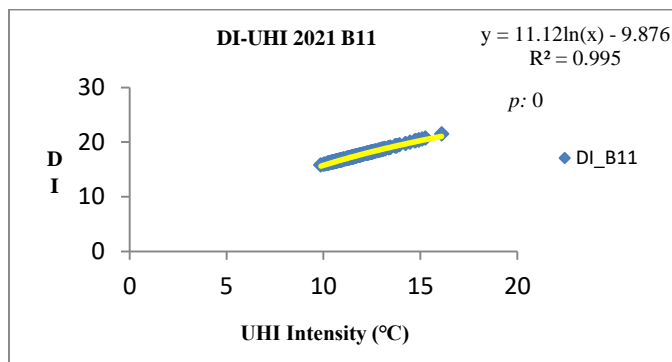
Graph 3.3.1(c)



Graph 3.3.1(d)



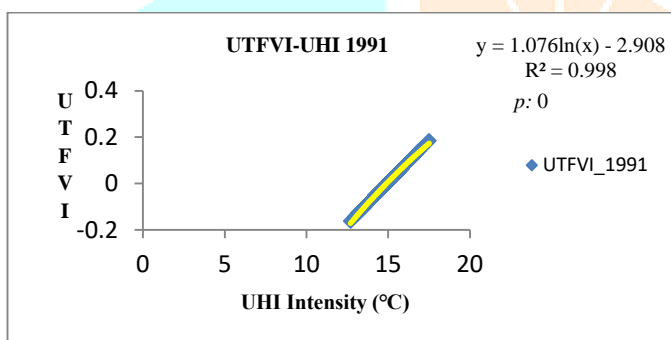
Graph 3.3.1(e)



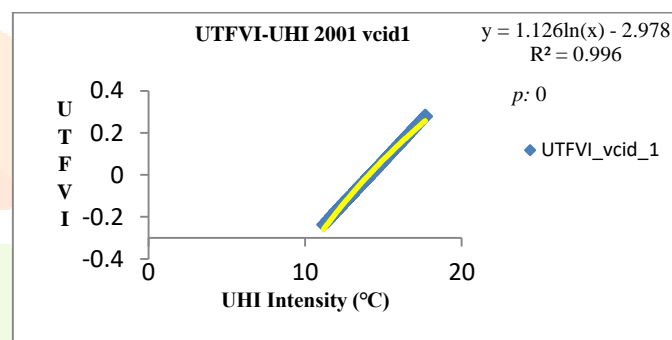
Graph 3.3.1(f)

Human discomfort was significantly impacted by urban heat islands intensity in 1991, 2001, 2011, and 2021, according to the graphs 3.3.1(a), 3.3.1(b), 3.3.1(c), 3.3.1(d), 3.3.1(e), and 3.3.1(f)

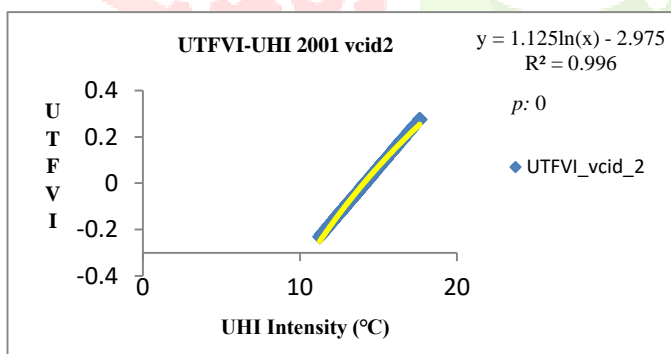
Therefore, it is evident from the aforementioned graphs that Urban Heat Island (UHI) Intensity has a significant impact on human comfort (having a maximum gradient for 1991 and a minimum for 2021 [B11]).



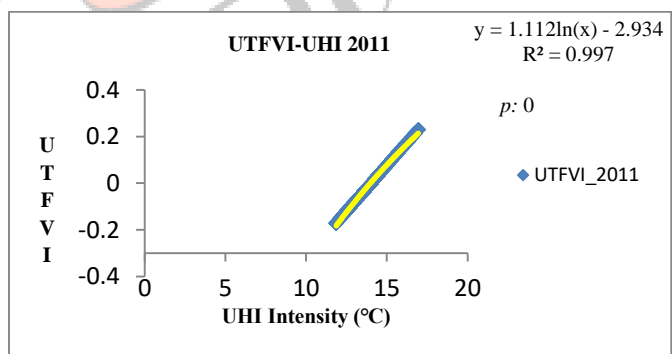
Graph 3.3.2(a)



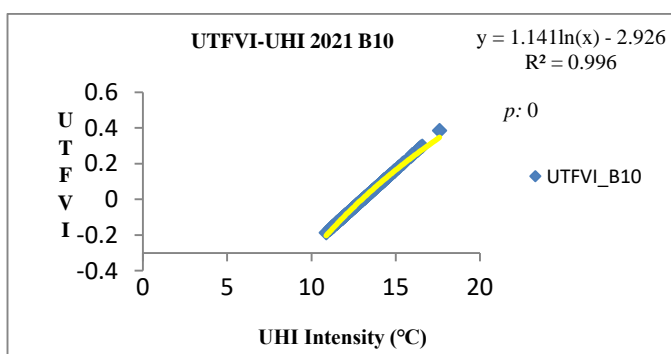
Graph 3.3.2(b)



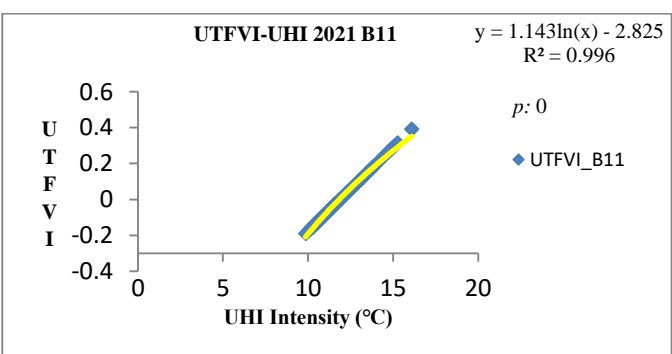
Graph 3.3.2(c)



Graph 3.3.2(d)



Graph 3.3.2(e)



Graph 3.3.2(f)

The graphs 3.3.2(a), 3.3.2(b), 3.3.2(c), 3.3.2(d), 3.3.2(e), and 3.3.2(f) all demonstrate the significant impact that urban heat islands intensity have had on ecological evolution since 1991. The graphs 3.3.2 (e) and 3.3.2 (f) also demonstrate the significant impact that urban heat islands will have on ecological evolution by the year 2021.

Therefore, it is evident from the aforementioned graphs that Ecological Evolution is significantly impacted by Urban Heat Island (UHI) Intensity (having a maximum gradient for 2021 [B11] and a minimum for 1991), but it is trending in the opposite direction from Human Discomfort.

Discussion:

It is necessary to adopt methods of reducing urban heat island intensity due to the thermal impact on human comfort and ecological evolution. There are two main categories of methods:

Green space: According to K.R. Gunawardena et al., (2017), the greenspace can take the form of parks, street trees and verges, private gardens, the edges of transportation corridors, and vegetated roofs and facades. The plant community structure (Yiding et al., 2006) and leaf area (Allen, Tasumi, and Trezza, 2002) of a green area affect cooling and humidity levels. Due to its shading effect, the vegetation community with trees has a significant impact on cooling (Giridharan, Lau, Ganesan & Givoni, 2008). Therefore, the cooling strength and cooling distance decrease as the park's area decreases (Xiao-gang et al., 2008; Feyisa, Dons, & Meilby, 2014). These types of green space provides more and more comfort to human as it reduce the effect of heat due to evapotranspiration however it also provides shelter to many birds and by default protect from anthropogenic hazards.



When compared to other heat mitigation strategies, the cooling distribution in green spaces is most likely to be effective at reducing heat stress (Doick et al., 2014; K.R. Gurawardena et al., 2017). The distribution of vegetation (trees, shrubs, or grass), typically

in the following order: arbor > shrub > lawn (Bowen, Dexiang, Jianjun & Lin, 2005; Liangmai, Haixia, Dongyun, Jiyu, & Jianlong, 2007), as well as its heterogeneity (Gill et al., 2013; Doick and Hutchings, 2013), has a significant impact on the cooling from large scale bodies. Larger parks, on the other hand, allow for greater cooling transport into the surrounding urban fabric during high temperature periods (K.R. Gunawardena et al., 2017; Xiang et al., 2018). Due to evapotranspiration and tree shading, greenspace functions as a cool island (Heri Andoni, 2018). However, for better observable effects, the Differential equations should be converted into difference equations at the time of plantation (Andrade and Vieira, 2007; Hamada and Ohta, 2010). Such types of strategies of green space plantation can give more relaxable environment to humans and natural beings as well (Jo Barton and Mike Rogerson, 2017; Kate Douglas and Joe Douglas, 2021).

Blue Space: Coutts et al., (2012) suggest that City planners and urban managers should have regarded waterbodies such as lakes, ponds and rivers as crucial components of strategy to minimize urban heat stress. The term "urban blue space" or "urban waterbodies" refers to all substantial bodies of static or dynamic water found in urban areas (ARUP, 2014). The net effect of radiation balance, the climate factors that promote the conversion of sensible to latent heat (Hathway and Sharples, 2012) determines how effectively a bluespace can cool the specific area. In contrast, shallow waterbodies like ponds, swales, water gardens, etc. have a larger surface area and are less deep because they provide better cooling through extensive contact with the atmosphere, balance, and evaporative flux (Evans et al., 1998; Caissie, 2006).



Other methods for reducing the urban heat island effect include high albedo surfaces, reducing heat emissions from man-made objects (Al-mulali et al., 2012; Wang et al., 2016; Zhang, 2016); and designs and patterns of building clusters (Francesco De Luca, 2019; Ran Xiao, 2020) and by constructing green roofs and planting trees nearby (N.H. Wong et al., 2007; M. Fadhil et al., 2023) and by decreasing barren land area (Shweta Jain et al., 2020; M. Fadhil et al., 2023).

Conclusion: Urban Heat Island (UHI) Intensity has its significant concern because it affects human health and the ecological evolution of the study area taken into consideration. In the current context of urbanization, the human settlement pattern has undergone significant changes, which have had distinctive negative environmental effects and led to the intensification of urban economic activities and production leading to negative effect on

ecosystem. The techniques for mitigating UHI effects should therefore be adopted, and we should come up with some strong and self-disciplined strategies to solve issues like the significant heat effects of Indian cities, particularly for the Ganga-Yamuna Doab region where there is a large population and uncontrolled urban structures are taking place and man-made objects are increasing rapidly which ultimately increasing the numbers of Urban Heat Islands, and we should try our best to minimize the number of heat islands because it is all for about our future, especially for younger generation.

Acknowledgement:

The authors are grateful to the University Grants Commission (UGC) and Principal of D.A.V. Degree College, Kanpur for providing the necessary facilities for the successful completion of this research. The first author wishes to acknowledge the support received from the Council of Scientific & Industrial Research (CSIR), New Delhi, India for providing grant under CSIR NET-JRF fellowship (Ref No.455/CSIR-UGC NET DEC. 2016).

Conflicts of Interest: There is no conflict of interest at all by all authors.

References:

1. Aflaki A. et al. (2017) Urban Heat island mitigation strategies: A state-of-art review on Kuala Lumpur, Singapore and Hong Kong. *Cities*, 62, pp.131-145, doi.org/ 10.1016/j.cities.2016.09.003
2. Chakraborty T. et al. (2016) Understanding Diurnality and Inter-Seasonality of a sub-tropical Urban Heat Island. *Boundary-Layer Meteorology*, doi.org/10.1007/s10546-016-0223-0
3. District Census Handbook, 2011
4. F. Yuan and M. E. Bauer (2007) Comparison of Impervious Surface Area and Normalized Difference Vegetation Index as Indicators of Surface Urban Heat Island Effects in Landsat Imagery, *Remote Sensing of Environment*, vol. 106, no. 3, pp. 375–386, doi.org/10.1016/j.rse.2006.09.003.
5. Fadhil Mohammed et al. (2023) Mitigating urban heat island effects in urban environments: strategies and tools. *Earth and Environmental Science*, 1129, 012025 doi.org/10.1088/1755-1315/1129/1/012025
6. Gunawardena K.R. et al. (2017) Utilizing green and blue space to mitigate urban heat island intensity. *Science of Total Environment*. 584-585, pp.1040- 1055, doi.org/ 10.1016/j.scitotenv.2017.01.158
7. Grimmond C.S.B. and T.R. Oke (1998) Heat Storage in Urban Areas: Local Scale Observations and Evaluation of a Simple Model. *Journal of Applied Metrology*. Vol.38, pp. 922-940
8. J. S. Silva, R. M. da Silva, and C. A. G. Santos (2018) Spatiotemporal Impact of Land Use/Land Cover Changes on Urban Heat Islands: A Case Study of Paço do Lumiar, Brazil, *Building and Environment*, vol. 136, pp. 279–292, doi.org/10.1016/j.buildenv.2018.03.041
9. Jain Shweta et al. (2020) Urban heat island intensity and its mitigation strategies in the fast-growing urban areas. *Journal of Urban Management*, 9(1), pp. 54-66 doi.org/10.1016/j.jum.2019.09.004
10. Konopacki S. and Akbari H. 2002: Energy Savings of Heat-Island Reduction Strategies in Chicago and Houston. Lawrence Berkeley National Laboratory, pp.51
11. Lee Yeeyong et al. 2014 Overview of Urban Heat Island (UHI) phenomenon towards Human Thermal Comfort. *Journal of Environmental Engineering and Management* 16(9), doi.org/10.30638/eemj.2017.217
12. Naim Md. Nazmul Huda and Abdulla-Al-Kafy (2021) Assessment of Urban Thermal Field Variance Index and defining the relationship between land cover and surface temperature in Chattogram city: A remote sensing and statistical approach *Environmental Challenges*, 4, pp.100-107.
13. Rani Meenu et al. (2018) Multi-temporal NDVI and surface temperature analysis for Urban Heat Island inbuilt surrounding of sub-humid region: A case study of two geographical regions. *Remote Sensing Applications: Society and Environment* (10) 163-172, doi.org/10.1016/j.rsase.2018.03.007
14. Renard Florent et al. (2019) Evaluation of the Effect of Urban Redevelopment on Surface Urban Heat Islands *Remote Sens.* 11, 299; doi.org/10.3390/rs11030299

15. .Rosenzweig C, Solecki WD, Slosberg R, (2006): Mitigating New York city's heat Island with urban forestry, living roofs and light surfaces. New York state energy research and development authority report: 123
16. Sobrino José Antonio and Itziar Irakulis (2020) A Methodology for Comparing the Surface Urban Heat Island in Selected Urban Agglomerations Around the World from Sentinel-3 SLSTR Data Remote Sens. 2020, 12, 2052, doi.org/10.3390/rs12122052
17. Steeneveld G.J. (2014) Refreshing the role of open water surfaces on mitigating the maximum urban heat island effect. Landscape and Urban Planning. 121, pp. 92-96, doi.org/10.1016/j.landurbplan.2013.09.001
18. United Nations, Department of Economic and Social Affairs, Population Division (2019). World Urbanization Prospects: The 2018 Revision (ST/ESA/SER.A/420). New York: United Nations.
19. Wong N.H. et al. (2007) Environmental study of the impact of greenery in an institutional campus in the tropics. Building and Environment, 42(8), pp. 2249-2270
20. Xiao Ran (2020) Comparing and Clustering Residential Layouts Using a Novel Measure of Grating Difference. Nexus Network Journal, 2021(23), pp. 187-208. doi.org/10.1007/s00004-020-00530-z
21. Xiao Xiang Dong et al. (2018) The influence of the spatial characteristic of urban green space on the urban heat island effect in Suzhou Industrial Park. Sustainable Cities and Society. 40, pp. 428-439; doi.org/10.1016/j.scs.2018.04.002

